



Original article

Cisplatin resistance involves a metabolic reprogramming through ROS and PGC-1 α in NSCLC which can be overcome by OXPHOS inhibition

Alberto Cruz-Bermúdez^{a,*}, Raquel Laza-Briviesca^{a,1}, Ramiro J. Vicente-Blanco^{a,1},
Aránzazu García-Grande^b, María José Coronado^c, Sara Laine-Menéndez^d,
Sara Palacios-Zambrano^e, M. Rocío Moreno-Villa^a, Asunción Martín Ruiz-Valdepeñas^a,
Cristina Lendinez^a, Atocha Romero^a, Fernando Franco^a, Virginia Calvo^a, Cristina Alfaro^a,
Paloma Martín Acosta^{f,g}, Clara Salas^f, José Miguel García^a, Mariano Provencio^{a,**}

^a Servicio de Oncología Médica, Instituto de Investigación Sanitaria Puerta de Hierro-Segovia de Arana (IDIPHSA), Hospital Universitario Puerta de Hierro-Majadahonda, Madrid, Spain

^b Flow Cytometry Core Facility, Hospital Universitario Puerta de Hierro Majadahonda, Madrid, Spain

^c Confocal Microscopy Core Facility, Hospital Universitario Puerta de Hierro Majadahonda, Madrid, Spain

^d Mitochondrial and Neuromuscular Disease Laboratory, Instituto de Investigación Hospital “12 de Octubre” (i+12), Madrid, Spain

^e Departamento de Bioquímica, Instituto de Investigaciones Biomédicas “Alberto Sols” UAM-CSIC, Facultad de Medicina UAM, Madrid, Spain

^f Department of Pathology, Hospital Puerta de Hierro, Majadahonda, Madrid, Spain

^g Centro de Investigación Biomédica en Red de Cáncer (CIBERONC), Madrid, Spain

ARTICLE INFO

Keywords:

Chemotherapy
Chemoresistance
NSCLC
Metabolism
Metformin

ABSTRACT

Background: Platinum-based chemotherapy remains the standard of care for most lung cancer cases. However chemoresistance is often developed during the treatment, limiting clinical utility of this drug. Recently, the ability of tumor cells to adapt their metabolism has been associated to resistance to therapies. In this study, we first described the metabolic reprogramming of Non-Small Cell Lung Cancer (NSCLC) in response to cisplatin treatment.

Methods: Cisplatin-resistant versions of the A549, H1299, and H460 cell lines were generated by continuous drug exposure. The long-term metabolic changes, as well as, the early response to cisplatin treatment were analyzed in both, parental and cisplatin-resistant cell lines. In addition, four Patient-derived xenograft models treated with cisplatin along with paired pre- and post-treatment biopsies from patients were studied. Furthermore, metabolic targeting of these changes in cell lines was performed downregulating PGC-1 α expression through siRNA or using OXPHOS inhibitors (metformin and rotenone).

Results: Two out of three cisplatin-resistant cell lines showed a stable increase in mitochondrial function, PGC-1 α and mitochondrial mass with reduced glycolysis, that did not affect the cell cycle. This phenomenon was confirmed *in vivo*. Post-treatment NSCLC tumors showed an increase in mitochondrial mass, PGC-1 α , and a decrease in the GAPDH/MT-CO1 ratio. In addition, we demonstrated how a ROS-mediated metabolism reprogramming, involving PGC-1 α and increased mitochondrial mass, is induced during short-time cisplatin exposure. Moreover, we tested how cells with increased PGC-1 α induced by ZLN005 treatment, showed reduced cisplatin-driven apoptosis. Remarkably, the long-term metabolic changes, as well as the metabolic reprogramming during short-time cisplatin exposure can be exploited as an Achilles' heel of NSCLC cells, as demonstrated by the increased sensitivity to PGC-1 α interference or OXPHOS inhibition using metformin or rotenone.

Conclusion: These results describe a new cisplatin resistance mechanism in NSCLC based on a metabolic reprogramming that is therapeutically exploitable through PGC-1 α downregulation or OXPHOS inhibitors.

Abbreviations: CDDP, Cisplatin, cis-diamminedichloroplatinum(II); OXPHOS, Oxidative Phosphorylation; PGC-1 α , Peroxisome proliferator-activated receptor gamma coactivator 1-alpha; ROS, Reactive Oxygen Species; MIMP, Mitochondrial inner membrane Potential; PDX, Patient Derived Xenograft

* Corresponding author. Hospital Universitario Puerta de Hierro-Majadahonda, Calle Manuel de Falla, 1, Madrid, 28222, Spain.

** Corresponding author. Hospital Universitario Puerta de Hierro-Majadahonda, Calle Manuel de Falla, 1, Madrid, 28222, Spain.

E-mail addresses: acruz@idiphim.org (A. Cruz-Bermúdez), mariano.provencio@salud.madrid.org (M. Provencio).

¹ These authors contributed equally.

<https://doi.org/10.1016/j.freeradbiomed.2019.03.009>

Received 11 September 2018; Received in revised form 8 March 2019; Accepted 9 March 2019

Available online 14 March 2019

0891-5849/ © 2019 The Authors. Published by Elsevier Inc. This is an open access article under the CC BY-NC-ND license

(<http://creativecommons.org/licenses/by-nc-nd/4.0/>).

1. Background

Lung cancer is the most common cancer worldwide in terms of incidence (1.2 million new cases per year, accounting for 16.7% of the total cancer burden) and it is also the leading cause of cancer-related death in the world (19.4% of the total). In addition to the human cost, lung cancer has a high economic impact on both health services and society as a whole [1,2].

About 85%–90% of lung cancers diagnosis are non-small cell lung cancer (NSCLC). Present-day classification of NSCLC takes into account molecular alterations that may influence therapeutic decision. However, at the moment we still do not have a drug-targetable driver mutation identified for most NSCLC patients (near 85–90%) and thus, platinum-based chemotherapy remains the standard of care. Moreover, in that small percentage of patients with drug-targetable driver mutations cisplatin-based therapy is also the principal approach following targeted therapy [1,2].

On the other hand, although lung cancer treatments have progressed significantly during the past years [3], and even more recently with the appearance of immunotherapy, their cost-effectiveness compared with chemotherapy-based approaches will be an issue to address [4]. Thus, cisplatin remains the main drug for treating NSCLC [5]. Sadly, during treatment, chemoresistance is often developed or it has to be discontinued due to platinum toxicity limiting the clinical utility of this drug. Therefore, a better understanding of cisplatin molecular mechanisms of action and its resistance would greatly improve patients outcome.

The mechanisms of cisplatin resistance are complex, involving diverse strategies and pathways [5]. Although altered energetic metabolism is one of the cancer hallmarks [6], little has been shown in its role in chemoresistance [7].

Mitochondria are organelles known to be the powerhouse of the cell, responsible for the oxidative phosphorylation (OXPHOS). In this process the acetyl CoA from glycolysis or fatty-acid oxidation powers the tricarboxylic acid cycle (TCA) that generates reduced cofactors. These cofactors are able to transfer electrons to the OXPHOS system which, through a chain of redox reactions, finally reduce oxygen to water. Some of these reactions produce ROS as a byproduct [8]. Simultaneously, during this process, protons are pumped into the intermembrane space generating what is known as Mitochondrial Inner Membrane Potential (MIMP) that is finally dissipated through Complex V generating ATP.

The classic view of tumor's metabolism is the well-known Warburg effect. According to this theory, the tumor cells increase their aerobic glycolysis reducing the OXPHOS function in order to boost the supply of metabolic intermediates used in anabolic processes [9–11].

However, under some circumstances, tumor cells have the ability to adapt their metabolism to different environments and treatments, increasing adaptability and tumor resistance to therapies [7,8]. In this sense, an increase of the OXPHOS function has been described for some tumors, although there is no data for NSCLC and cisplatin. These adaptation processes may be performed by controlling the mitochondrial biogenesis, which is largely controlled by the transcriptional coactivator peroxisome proliferator-activated receptor gamma coactivator-1 alpha (PGC-1α). Theoretically, these metabolic changes open a therapeutic opportunity to target resistances by using metabolic inhibitors [12,13].

Metformin has aroused great interest over the last years due to its association with lower cancer incidence in type two diabetic patients and better overall survival in cancer patients [14]. Metformin is also an inhibitor of the complex I of the OXPHOS system. However, its role in OXPHOS modulation in relation with cisplatin has not been studied in NSCLC. Furthermore, metformin is a drug widely used for its anti-diabetic properties, and has been in use for more than fifty years without any important interactions with most cancer treatments. These characteristics make metformin really interesting for cancer therapy

due to its possible application, which would be much more direct avoiding most of the limiting steps in drug-development [15].

In this study we generated cis-diamminedichloroplatinum(II) (CDDP)-resistant versions of 3 different NSCLC cell lines (A549, H1299 and H460) to characterize the stable metabolic changes associated with increased CDDP resistance and also to evaluate the early changes in response to CDDP treatment. Patient Derived Xenografts (PDX) models treated with CDDP and paired pre- and post-treatment tumor biopsies of NSCLC patients were also studied. Finally, we used these changes as a therapeutic target of CDDP-resistant cells. This work provides a new insight into cisplatin resistance mechanism in NSCLC cells that may lead to the design of novel therapeutic approaches.

2. Methods

2.1. Patients, cell lines and reagents

Stage III NSCLC patients who had pre- and post-treatment paired samples were retrospectively selected. A549, H1299, and H460 were obtained from the ATCC. All cells were cultured routinely in DMEM, with 10% Fetal Bovine Serum (FBS) and Penicillin Streptomycin (Gibco). Cisplatin (Accord, 1 mg/mL) was obtained from the Oncology Service of the Hospital Puerta de Hierro Majadahonda. ZLN005, Rotenone, CCCP, and NAC were purchased from Sigma.

2.2. Cell viability assays

Cells were set up at 3×10^3 cells per well of a 96-well plate and were cultured in DMEM overnight. The next morning the medium was refreshed with DMEM containing the different treatments according to figure legends. Cell viability was assayed by Cell Counting Kit-8 (CCK-8) (Dojindo EU GmbH, Munich, Germany) according to the manufacturer's protocol.

2.3. Glucose and galactose growth curves

Cell growth was evaluated after seeding 6 well plates at a density of 25,000 cells/well and growing the cells for 4 days in DMEM containing either 4.5 g/L glucose or 0.9 g/L galactose. The cells were harvested and counted every 24 h. Population doubling times were calculated using *Doubling Time Software v1.0.10* (<http://www.doubling-time.com>). Assays were performed by duplicate in at least 3 independent experiments.

2.4. Cell cycle, MIMP, mitochondrial mass and ROS using fluorescent molecular probes

Cell cycle was determined using Vybrant™ DyeCycle™ Violet Stain. Cytoplasmic ROS were assessed using 2',7'-dichlorodihydrofluorescein diacetate (H₂DCFDA). 1 h of serum starvation was used as positive control for ROS measurements. The mitochondrial inner membrane potential (MIMP) was evaluated using tetramethyl rhodamine ester (TMRE). CCCP was used as a negative control for MIMP assesment. The mitochondrial mass was evaluated using Mitotracker Green FM (MTG). All the fluorescent probes were purchased from Molecular Probes®.

After addition of the fluorophores (5 μM Vybrant, 30 μM DCFHDA, 100 nM TMRE, 100 nM MTG) and incubation at 37 °C for 30 min in the dark, the cells were collected in DMEM and analyzed immediately with a Cytomic FC500 MPL flow cytometer (Beckman Coulter). Forward and side scatter were used to gate the viable population of cells, and the mean fluorescence intensity was determined with MXP software (Beckman Coulter). Experiments were performed in duplicate on at least three independent passages.

2.5. Glucose consumption

The glucose consumption was determined through the measurement of the concentration present in the cell medium over time. To do this, 3×10^5 cells were seeded in a 6-well plate. The next day, the medium was removed and 500 μ L of fresh DMEM was added. After 6 h of incubation the concentration present in the medium was determined. To measure the concentration of glucose in the medium, an Accu-Check Performa glucometer (Roche) was calibrated and used. Both the samples and the standard curve (500–0.15 g/L) were diluted $\frac{1}{2}$ with distilled water before the measurement. The results are shown as mg of glucose consumed at 6 h. At least three independent measurements were obtained to generate the mean.

2.6. Oxygen consumption

The oxygen consumption of intact cells was measured in DMEM at 37 °C using a Clark-type oxygen electrode (Hansatech Instruments). Basal respiration was calculated as the oxygen consumption rate minus the non-mitochondrial respiration after KCN 1 mM addition. At least three independent measurements were obtained to generate the mean.

2.7. OXPHOS blue native PAGE

Mitochondria were purified from cell cultures as described [16]. Protein concentrations were determined using the microBCA protein kit (Thermo Scientific). To obtain native mitochondrial proteins, pellets were solubilized with 4 g digitonin (Sigma) per gram of protein in 1.5 M aminocaproic acid, 50 mM Bis-Tris, pH 7.0. Blue native electrophoresis was performed as described [17]. NDUFA9 (Abcam, ab14713) was used for the immunodetection of OXPHOS supercomplexes I + III₂ + IV. SDHA (Abcam, ab14715) was used for normalization. Quantification of 4 different blots from 2 different extracts was done using ImageJ.

2.8. Immunofluorescence

Cells were fixed with paraformaldehyde 4%, incubated overnight with TOM20 antibody (Santa Cruz Biotechnology, sc-17764, 1/50). Alexa Fluor 488 anti-mouse (Invitrogen Life Technologies, 1/500) was used as secondary antibody. Nuclei were stained with Topro-3 (Invitrogen Life Technologies, 1/1000). Five images of each sample were collected with a TCS SP5 confocal microscope (Leica Microsystems) equipped with 20 \times HCX PL APO (0.7 numerical aperture). Two channels were acquired sequentially with the following excitation and emission parameters: (488 nm, 500–540 nm) for TOM20 signal, and (633 nm, 645–750 nm) for Topro-3. Data processing and quantification of fluorescence signal were performed with LASER SOFTWARE VERSION 2.6.07266.

2.9. mRNA expression analysis

The RNA from cells was extracted using the “RNeasy mini Kit with DNase” (Qiagen). The RNA from FFPE tumors was extracted using the High Pure FFPE RNA isolation kit (Roche). The cDNA was synthesized using the “NZY First-Strand cDNA Synthesis Kit” (NZYtech). PGC-1 α (Hs01016719_m1) LDHA (Hs01378790_g1), MCT4 (Hs00358829_m1), GAPDH (Hs02758991_g1), MT-CO1 (Hs02596864_g1) mRNA levels were measured by qRT-PCR using Taqman[®] gene expression assays. TBP (Hs00427621_m1) was used as endogenous control [18].

2.10. Western blotting

Catalase, MnSOD, AIF and Bcl2 expression was analyzed on cell extracts using specific antibodies from Sigma (C0979), Millipore (06–984) Abcam (ab32516) and SantaCruz (sc-7382), respectively. Immunodetection of γ -Tubulin (Sigma, T6557) was used as protein

loading control. Appropriate horseradish peroxidase coupled secondary antibodies were used and peroxidase activity was assessed by enhanced chemoluminescence (Amersham).

2.11. Patient derived xenograft models

Four different PDX models from four NSCLC patients were generated as described previously [19]. All the treatments were carried out in mice from passage two with bilateral palpable tumors. At least two mice per group were intraperitoneal injected with 2.5 mg/kg CDDP or vehicle two times per week in non-consecutive days. After the treatments the animals were euthanized and the tumors were collected.

2.12. siRNA transfection

Cells were transfected 24 h prior to experiments with Silencer[™] Select siRNA targeted to PGC-1 α (s21394, sequence 5' > 3': CCUGU UUGAUGACAGCGAAAtt) and nontargeting control (Silencer[™] Select Negative Control No. 1) using Lipofectamine RNAiMAX according to the manufacturer's instructions (Thermo Scientific).

2.13. Apoptosis measurement

Cells were seeded in a 24-well plate in DMEM. The next day, the medium was changed to DMEM or DMEM containing different treatments (5 μ M CDDP and/or 20 μ M ZLN005). After 48 h of treatments, apoptosis was evaluated by flow cytometry using the Annexin V, FITC Apoptosis Detection Kit (Dojindo) and by confocal microscopy using the DeadEnd[™] Fluorometric TUNEL system (Promega).

For flow cytometry studies, the cells were harvested, washed twice in PBS and resuspended in 50 μ L of 10-fold diluted Annexin V binding solution. 1 μ L of Annexin V-FITC conjugated and Propidium Iodide were added to the cells and incubated for 15 min at room temperature. Finally, the cells were additionally diluted with 150 μ L of 10-fold diluted Annexin V binding solution and immediately analyzed by flow cytometry. Forward and side scatter were used to gate the population of cells. The graph bars represent the mean percentage of Annexin positive cells from 4 measurements.

For confocal microscopy studies, the cells were first washed twice in PBS, fixed 20 min at 4 °C in paraformaldehyde 4% and labeled according to manufacturer's instructions. TO-PRO-3 was used as counterstain to visualize all nuclei.

2.14. Statistics

The results were presented as the mean \pm SD (Standard deviation). Unpaired two-tailed Student's t-test was used for statistical analysis among groups. For multiple comparisons in Fig. 5 (Supplementary Table 1) ANOVA with Tukey's post-hoc test was carried out. Differences were considered to be statistically significant when the p-value was < 0.05 (* = $P \leq 0.05$, ** = $P \leq 0.01$, *** = $P \leq 0.001$).

3. Results

3.1. Generation of cisplatin resistant cell lines

As a first step in the study of metabolic changes associated with cisplatin resistance in NSCLC, our goal was to obtain CDDP-resistant cell lines.

Thus, starting from three of the most common NSCLC cell lines from different origins (A549 primary tumor, H1299 lymph node and H460 pleural effusion), resistant versions were obtained after three months of treatment with 5 μ M CDDP. After this selection process, cells were evaluated for their vulnerability to CDDP treatment (Fig. 1A–C) and their IC₅₀ were calculated. As might be expected, the results showed that the continuous CDDP treatment led to the development of an

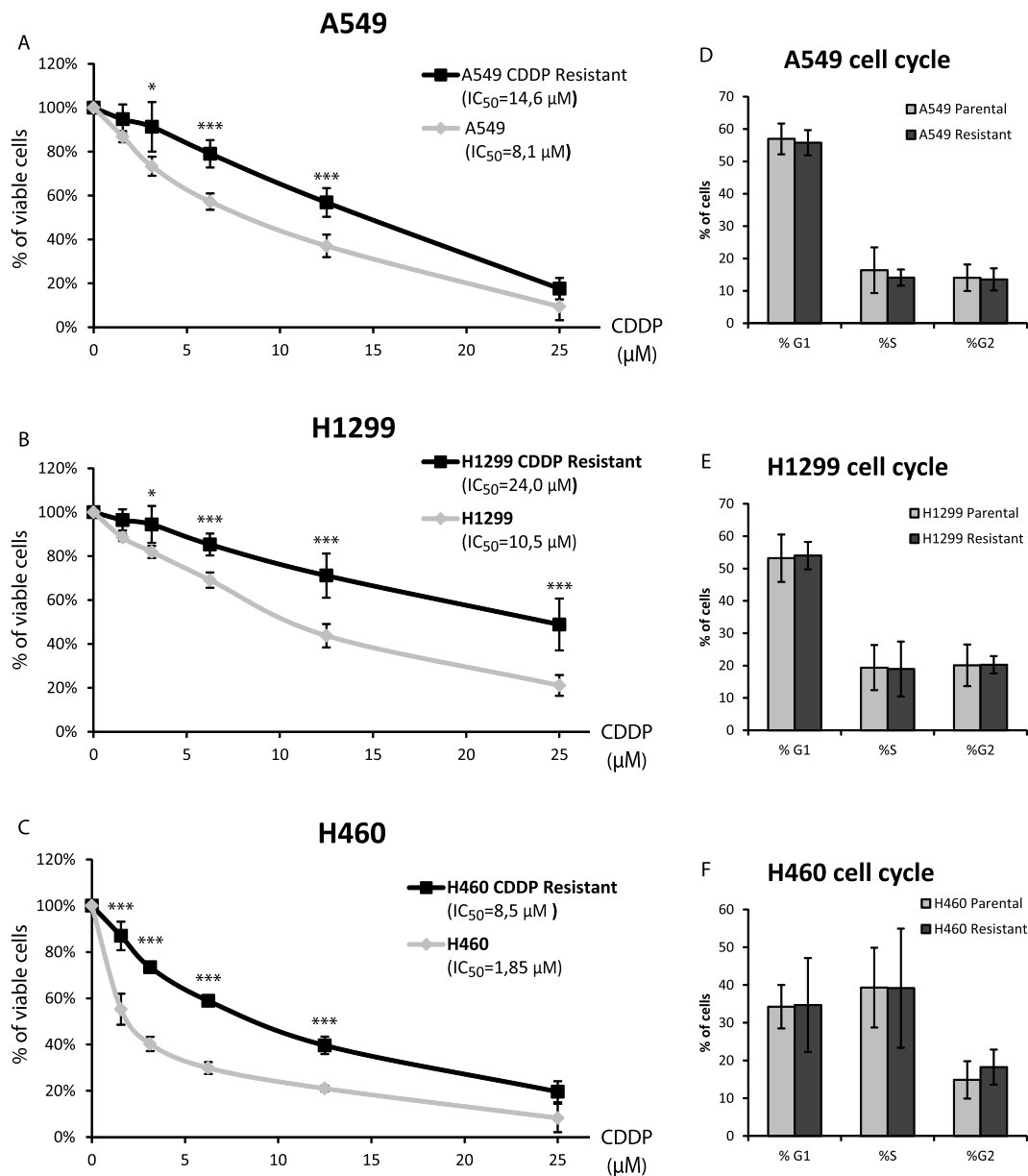


Fig. 1. Generation of CDDP-resistant cell lines. After continuous treatment of the cell lines (A) A549, (B) H1299, and (C) H460 with 5 μM CDDP, resistant versions of the cell lines were obtained. The graphs represent the percentage of viable cells (Y-axis) after 48 h of different CDDP treatments (X-axis) relative to untreated cells. Cell cycle analysis for parental and CDDP-resistant cell lines (D–F). Data are means from at least three different experiments. Error bars indicate standard deviation. Student's t-test p-value was considered to be statistically significant when was < 0.05 (* = $P \leq 0.05$, ** = $P \leq 0.01$, *** = $P \leq 0.001$).

increased resistance in the three cell lines, similarly to what happens in patients. Significant differences were seen in all the 3 cell lines from 3 μM to 12 μM cisplatin dose. Following experiments were done with 5 μM of cisplatin dose.

Since CDDP affects the DNA replication process, in order to exclude that the continuous CDDP treatment would have selected for cells with a more quiescent phenotype and metabolism, we studied the cell cycle of parental and CDDP-resistant cells. The results showed no differences in any of the cell cycle phases (G1, S, G2) between parental and CDDP-resistant cell lines (Fig. 1D–F). There were also no differences in the rate of proliferation during their handling in cell culture (data not shown).

3.2. Cisplatin resistant cell lines show an increased oxidative metabolism and mitochondrial biogenesis

Once we had three diverse NSCLC cellular models for resistance to

CDDP treatment, we proceed to characterize the metabolic changes associated to this stable increase in CDDP resistance (Fig. 2).

The vast majority of tumor cells show an altered balance between glycolytic and mitochondrial function. To analyze the glycolytic capacity of the cells, the glucose consumption from the cell media was measured. A decrease in glucose consumption was observed for the cell lines H1299 and H460 CDDP-resistant compared to their parental versions, but no differences were detected between parental and CDDP-resistant A549 cells (Fig. 2A). In a similar way, this reduction in glucose consumption was accompanied by a downregulation of LDHA, MTC4 and GAPDH mRNA levels, reinforcing the idea of a reduced glycolysis in H1299 and H460 CDDP-resistant cell lines (Supplementary Figure 1).

On the other hand, we measured the mitochondrial inner membrane potential (MIMP) since it is a good surrogate of the mitochondrial function. The results showed a significant increase in the MIMP compared to the parental cell lines for the H1299 and H460 CDDP-resistant

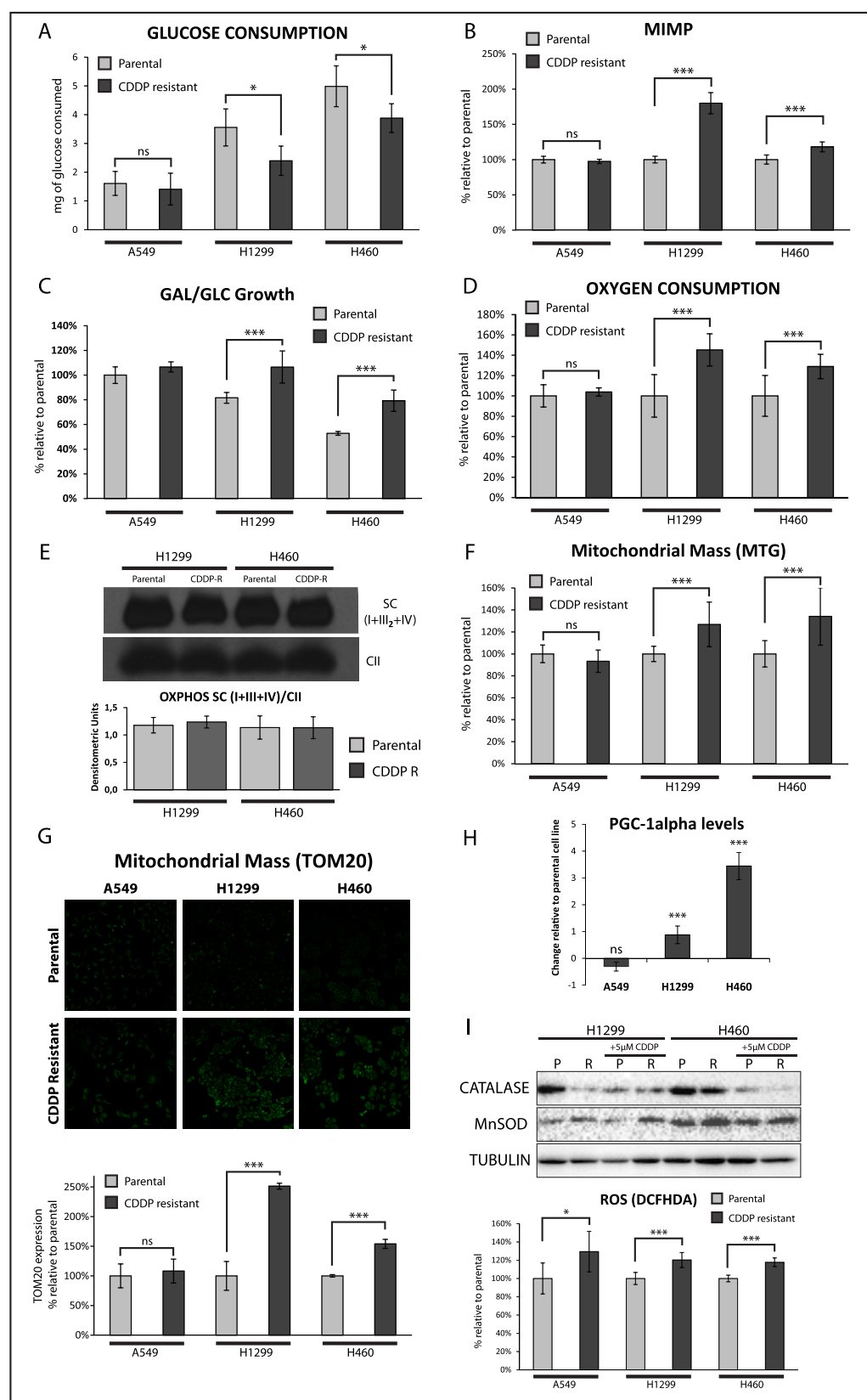


Fig. 2. Metabolic reprogramming in CDDP resistant cell lines. (A) Glucose consumption of cell lines. (B) Mitochondrial inner membrane potential was measured by flow cytometry with the fluorescent probe TMRE. (C) Relationship between the growth rate in galactose and glucose of the parental cell lines and resistant to CDDP, an increase in this ratio is indicative of an increase in OXPHOS function. (D) Oxygen consumption of intact cells was measured using a Clark-type electrode. (E) BN-PAGE of OXPHOS super-complexes in H1299 and H460 cells. (F–G) Mitochondrial Mass measured by Mitotracker Green and TOM20 Immunofluorescence. (H) Relative PGC1α mRNA levels for CDDP-resistant compared to parental cell lines. (I) Upper panel, Catalase and MnSOD levels measured by Western blot. “P” and “R” letters indicate Parental and Resistant cell lines. Lower panel, relative ROS levels measured using the fluorescent probe DCFHDA. Data are means from at least three different experiments and are represented as percentage of their respective parental cell line. Student’s t-test p-value was considered to be statistically significant when was < 0.05 (* = $P \leq 0.05$, ** = $P \leq 0.01$, *** = $P \leq 0.001$).

cell lines, but not for the A549 CDDP-resistant cell line (Fig. 2B).

To confirm that there was a change in the oxidative metabolism and not only in the MIMP that could be produced by other mechanisms, we decided to measure the galactose to glucose (Gal/Glu) growth ratio, indicative of the OXPHOS capacity of the cells (Fig. 2C), and the oxygen

consumption of these cells using a Clark-type oxygen electrode (Fig. 2D). Similarly to MIMP, the results showed an increase of the Gal/Glu growth ratio oxygen consumption for the H1299 and the H460 CDDP-resistant cell lines, although no differences were seen for the A549 cells.

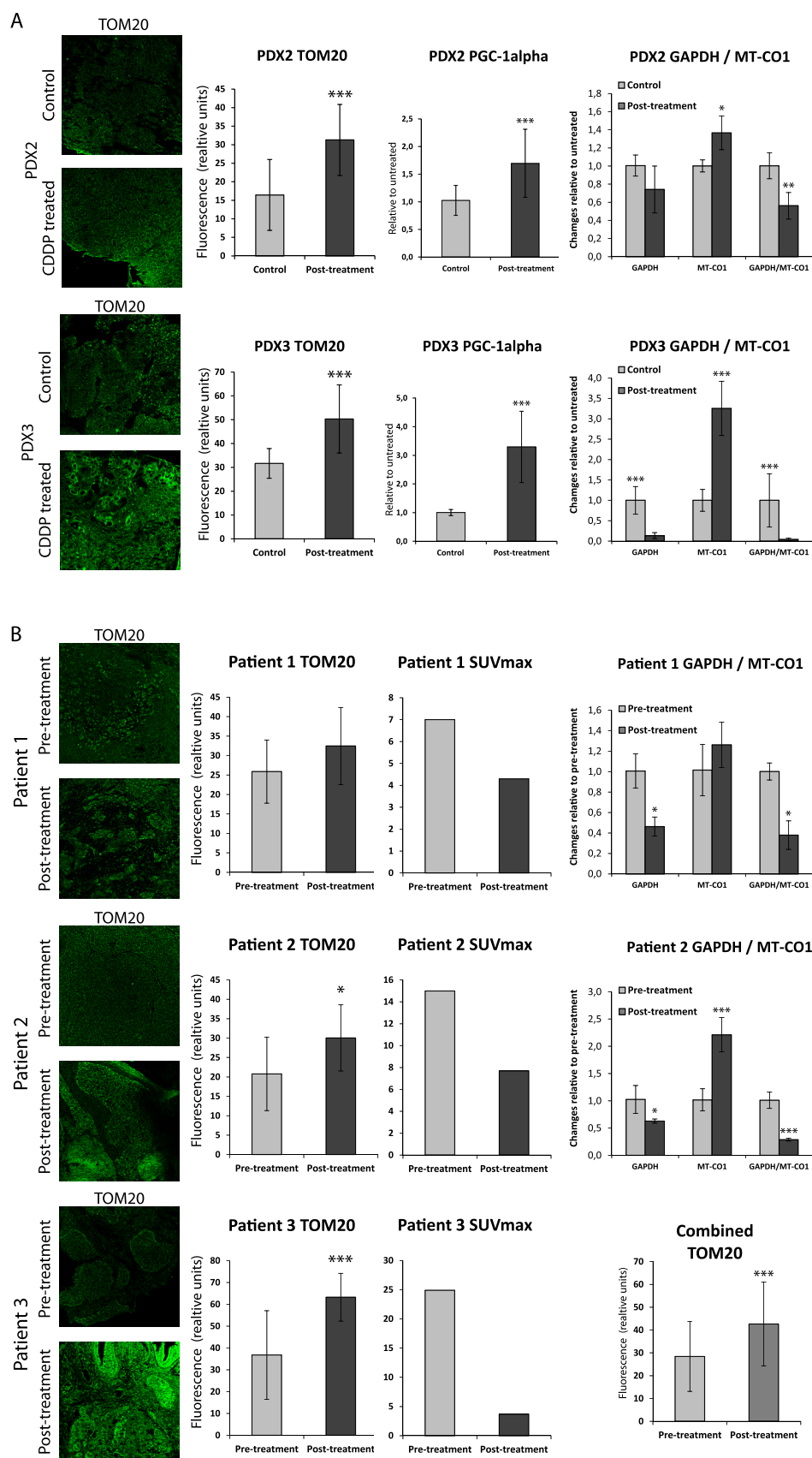
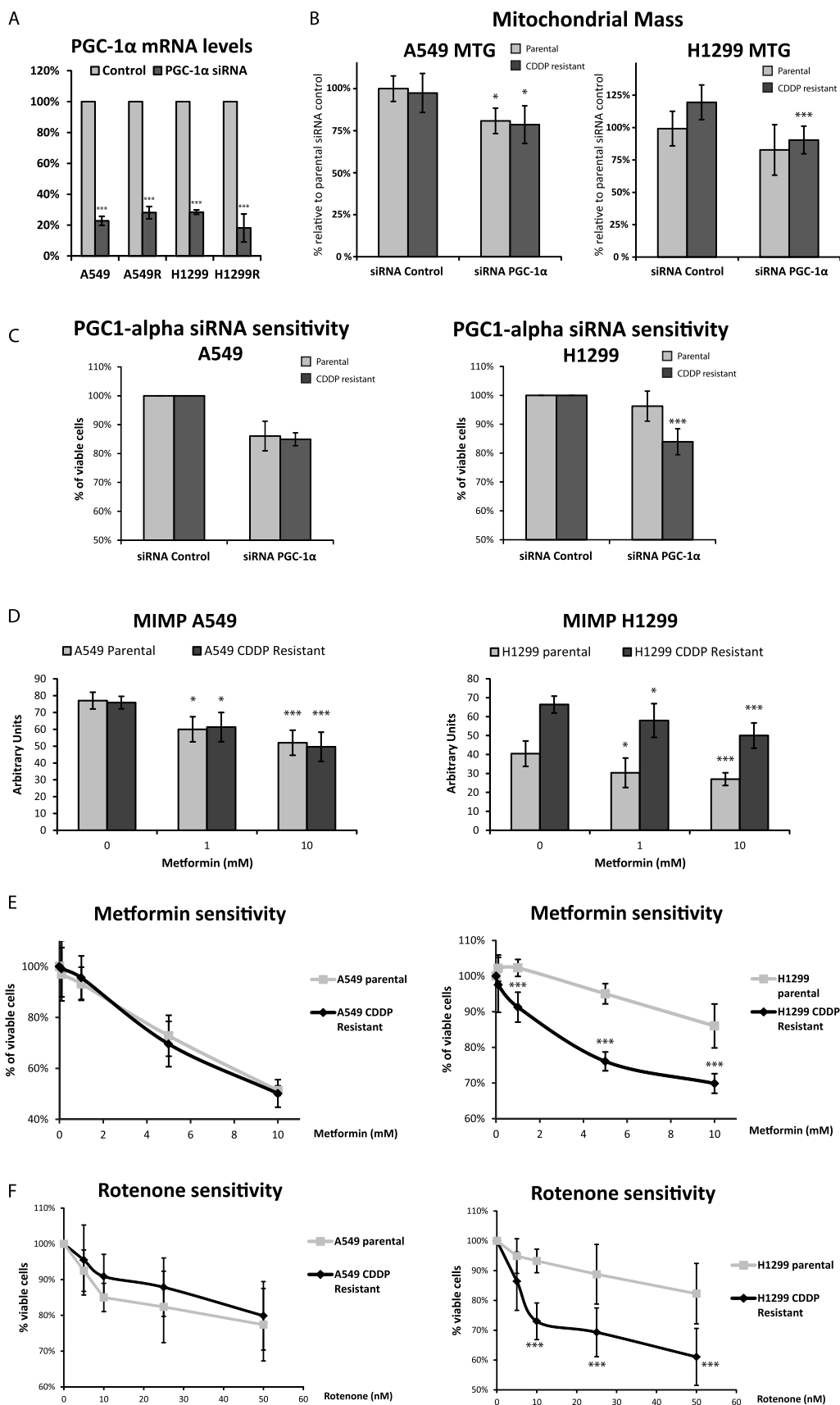


Fig. 3. Metabolic changes associated to Cisplatin treatment in PDX models and Patients biopsies. PGC-1 α mRNA, TOM20 and GAPDH/MT-CO1 levels relative to untreated controls for tumors obtained from PDX2 and PDX3 models (A). Analysis of NSCLC pre- and post-treatment tumor biopsies analysing TOM20, SUVmax and GAPDH/MT-CO1 ratio levels (B). Error bars indicate standard deviation. Student's t-test p-value was considered to be statistically significant when was < 0.05 (* = $P \leq 0.05$, ** = $P \leq 0.01$, *** = $P \leq 0.001$).



(caption on next page)

Fig. 4. Cisplatin resistance increase Metformin, Rotenone and PGC-1 α siRNA sensitivity. (A) PGC-1 α mRNA interference levels (B) PGC1 α siRNA interference decreases the Mitochondrial mass measured with MTG. (C) PGC-1 α siRNA sensitivity in parental and CDDP resistant cells (D) Metformin treatment reduces the MIMP in both A549 and H1299 cell lines, regardless of their CDDP resistance. (E and F) Metformin and rotenone sensitivity was evaluated for the A549 and H1299 parental cell lines and for their respective CDDP resistant versions. The graphs represent the percentage of viable cells (Y-axis) after 48 h of different metformin treatments (X-axis). Data are means from at least three different experiments and are represented as percentage of untreated cells. Error bars indicate standard deviation. Student's t-test p-value was considered to be statistically significant when was < 0.05 (* = $P \leq 0.05$, ** = $P \leq 0.01$, *** = $P \leq 0.001$).

To explain the mechanism behind the increase in MIMP and oxygen consumption, we studied the levels of OXPHOS complexes by BN-PAGE in H1299 and H460 cell lines in which there was a net increase in OXPHOS function (Fig. 2E). Strikingly, the results showed no significant differences in the amount of mitochondrial supercomplexes I + III₂ + IV. An explanation for this contradiction (increased oxygen consumption and MIMP but no changes in the amount of complexes) could be an increase of mitochondrial biogenesis. In this way, the mitochondrial network would harbor the same density of OXPHOS complexes but having more mitochondrial mass, the total amount of OXPHOS complexes per cell would be higher.

To test this hypothesis, we measured the levels of mitochondrial mass using the molecular probe Mitotracker Green (MTG) (Fig. 2F), as well as through immunofluorescence using TOM20 antibody (Fig. 2G). The results showed an increase of the mitochondrial mass for the CDDP-resistant H1299 and H460 cell lines. On the contrary, no changes were observed for the CDDP-resistant A549 cell line. Interestingly, this cell line also did not show an increase in the OXPHOS function.

These results were completed with a gene expression analysis for PGC-1 α , an oxidative stress inducible regulator of mitochondrial biogenesis (Fig. 2H). The expression levels for PGC-1 α were significantly increased in the H1299 and H460 CDDP-resistant cell lines compared to their parental cells. However, no changes were observed for the A549 CDDP-resistant cell line, similarly to that observed for mitochondrial mass, MIMP and oxygen consumption.

To check if the increase of PGC-1 α could lead to a reduction in the oxidative stress and therefore participate as resistance mechanism, we evaluated the levels of antioxidant proteins and also the steady state ROS levels (Fig. 2I). The immunoblot showed an increased mitochondrial superoxide dismutase (MnSOD), but reduced catalase levels, in H1299 and H460 CDDP-resistant cells fully consistent with the observed increase in the steady state levels of ROS, mainly H₂O₂, measured with DCFHDA. However, the results showed an increase in ROS levels for the all the CDDP-resistant cell lines, regardless of their PGC-1 α levels or the change in OXPHOS metabolism. These results would suggest that the antioxidant capacity of this cells do not participate in the increased CDDP-resistance. If this were the case, it would be more logical to observe lower levels of ROS in the CDDP-resistant cell lines.

3.3. Cisplatin treatment induces an increase in mitochondrial mass in PDX models and patients tumors

To confirm the results in cell lines, we decided to analyze whether this metabolism change occurred in a similar way in patient derived xenograft (PDX) models. Four PDX models from four NSCLC patients were generated.

Mice were randomly distributed in two groups, controls and CDDP-treated and PGC-1 α levels were evaluated (Fig. 3A). Tumors from two out of four PDX showed an increase in PGC-1 α levels (PDX2 and PDX3) after CDDP treatment. No differences were seen for PDX4 and PDX1 (Supplementary Figure 2). Additionally, for PDX2 and PDX3, mitochondrial mass was evaluated by Immunofluorescence of TOM20 and the ratio of GAPDH/MT-CO1 mRNA was calculated. In concordance with their increased PGC-1 α levels, there was a significant increase in mitochondrial mass as well as a reduction in the GAPDH/MT-CO1 ratio after CDDP treatment.

In addition, we decided to analyze whether this change could also be observed in pre- and post-treatment tumor biopsies of NSCLC

patients. Due to the difficulty of obtaining this type of paired pre- and post-treatment samples, stage III NSCLC patients were selected since their treatment is based in platinum doublet and their clinical routine includes a pre-treatment diagnostic biopsy and a post-treatment surgical biopsy. However, from ten patients only three samples were retrieved with enough material for the analysis. From all patients that were tested, an increase in the levels of mitochondrial mass was observed after CDDP treatment in the tumor cells, although this increase only was statistically significant in two of them (Fig. 3B). Anyhow, when the data from the three patients are combined, significative differences are observed.

Furthermore, FDG-PET images of these patients were available for pre- and post-treatment phases. From these images the SUVmax was calculated in both timepoints, showing a decrease of this parameter after treatment. Moreover, when possible due to biopsies size, RNA was extracted and the GAPDH/MT-CO1 mRNA ratio was calculated. The results from Patient 1 and Patient 2 show a decrease in GAPDH with and increase in MT-CO1 mRNA levels, which leads to a significant decrease in the GAPDH/MT-CO1 mRNA ratio.

3.4. Metabolic targeting of parental and CDDP-resistant NSCLC cells using PGC-1 α siRNA or OXPHOS inhibitors

The OXPHOS function characterization would indicate that the increase of mitochondrial biogenesis and OXPHOS function is a common phenomenon in cell lines, PDX and patients treated with CDDP. Following this hypothesis, we investigated if this group of CDDP-resistant cells with enhanced OXPHOS function could be targeted with the siRNA downregulation of PGC-1 α as well as using drugs that acts inhibiting the mitochondrial function.

For these studies we worked with the cell line H1299 since its CDDP-resistant version is the one that showed a greater increase of the MIMP. We used the cell line A549 as a negative control for which this phenomenon was not found.

First all of, we tested if the downregulation of PGC-1 α was able to reduce the mitochondrial mass. Using specific siRNA against PGC-1 α , we reached approximately a 70–80% reduction of PGC-1 α expression compared to control siRNA (Fig. 4A). In these conditions, the PGC-1 α interference reduced the mitochondrial mass measured with MTG in all the cell lines. Interestingly, the reduction for the parental H1299 line was not statistically significant, thus decreasing the differences in mitochondrial mass levels between parental and resistant when PGC was silenced (Fig. 4B).

Afterward, we measured the cell's sensitivity to PGC-1 α downregulation (Fig. 4C). The interference of PGC-1 α decreases the cell viability in all the cases, however this effect was significantly higher for the H1229 CDDP resistant cell line compared to its parental version. On the other hand, no differences in PGC-1 α interference sensitivity were found between parental and CDDP resistant A549 cell lines.

Secondly, we tested if the antidiabetic drug, metformin, was capable of reducing the MIMP of the cell lines. The addition of metformin to the A549 and H1299 cell lines decreased their MIMP regardless of their CDDP resistance (Fig. 4D).

After that, we evaluated the effect of different metformin concentrations on the viability of the parental and CDDP resistant cells (Fig. 4E). The results show a decrease in cell viability with increasing metformin concentrations. Remarkably, this effect is much greater in the case of the H1299 CDDP resistant cell line compared to its parent

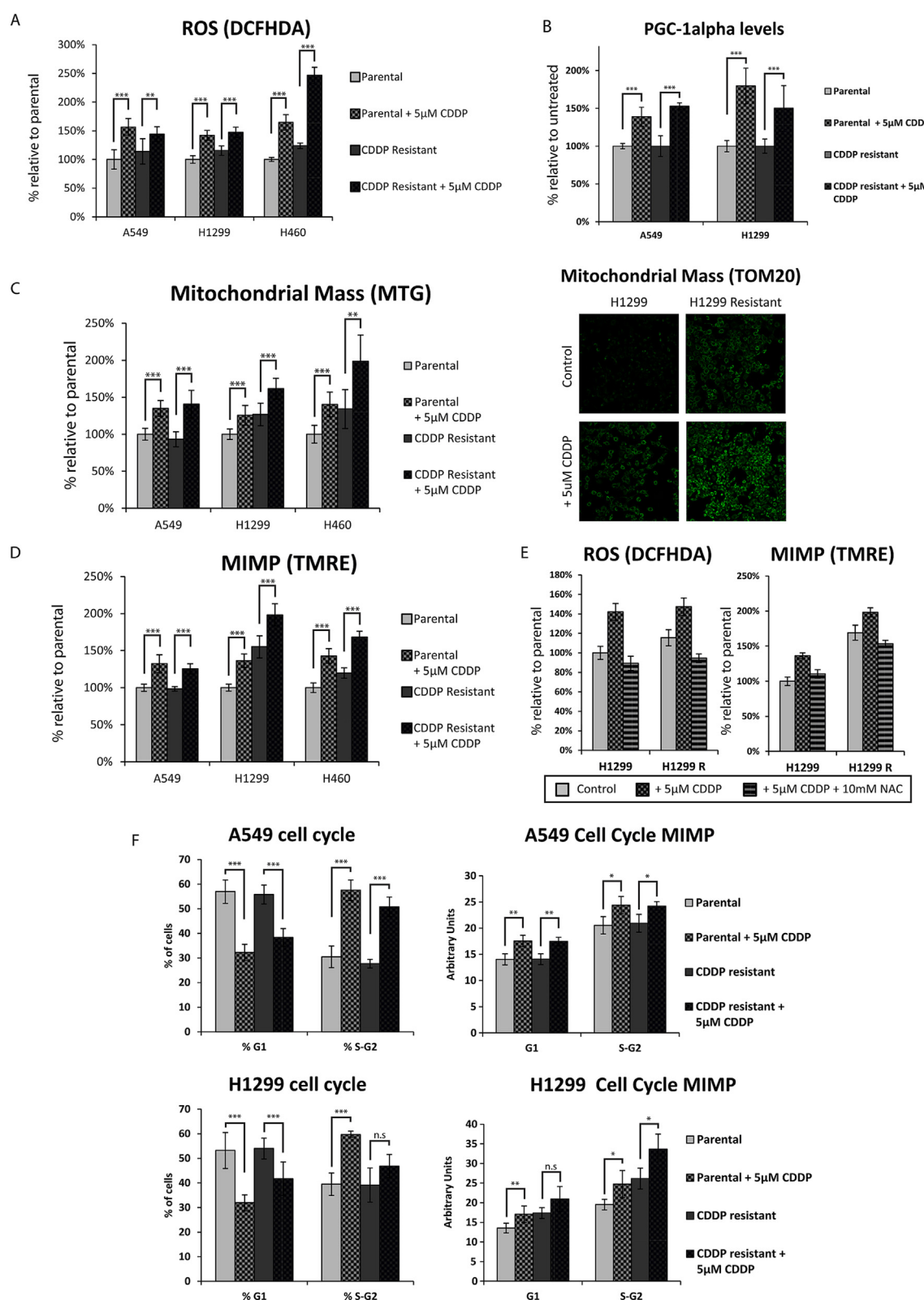


Fig. 5. Changes in MIMP and ROS in early response to CDDP treatment. Parental and CDDP resistant cell lines were treated with 5 μ M CDDP. Changes in ROS (A), PGC1- α levels (B), Mitochondrial Mass (C) and MIMP (D) were evaluated. Effect of concomitant 10 mM NAC in ROS and MIMP changes induced by CDDP treatment at 24 h (E). Cell cycle analysis and MIMP during CDDP treatment (F). Bars are means from at least three different experiments and are represented as percentage of untreated parental cells. Error bars indicate standard deviation. Student's t-test p-value was considered to be statistically significant when was < 0.05 (* = $P \leq 0.05$, ** = $P \leq 0.01$, *** = $P \leq 0.001$).

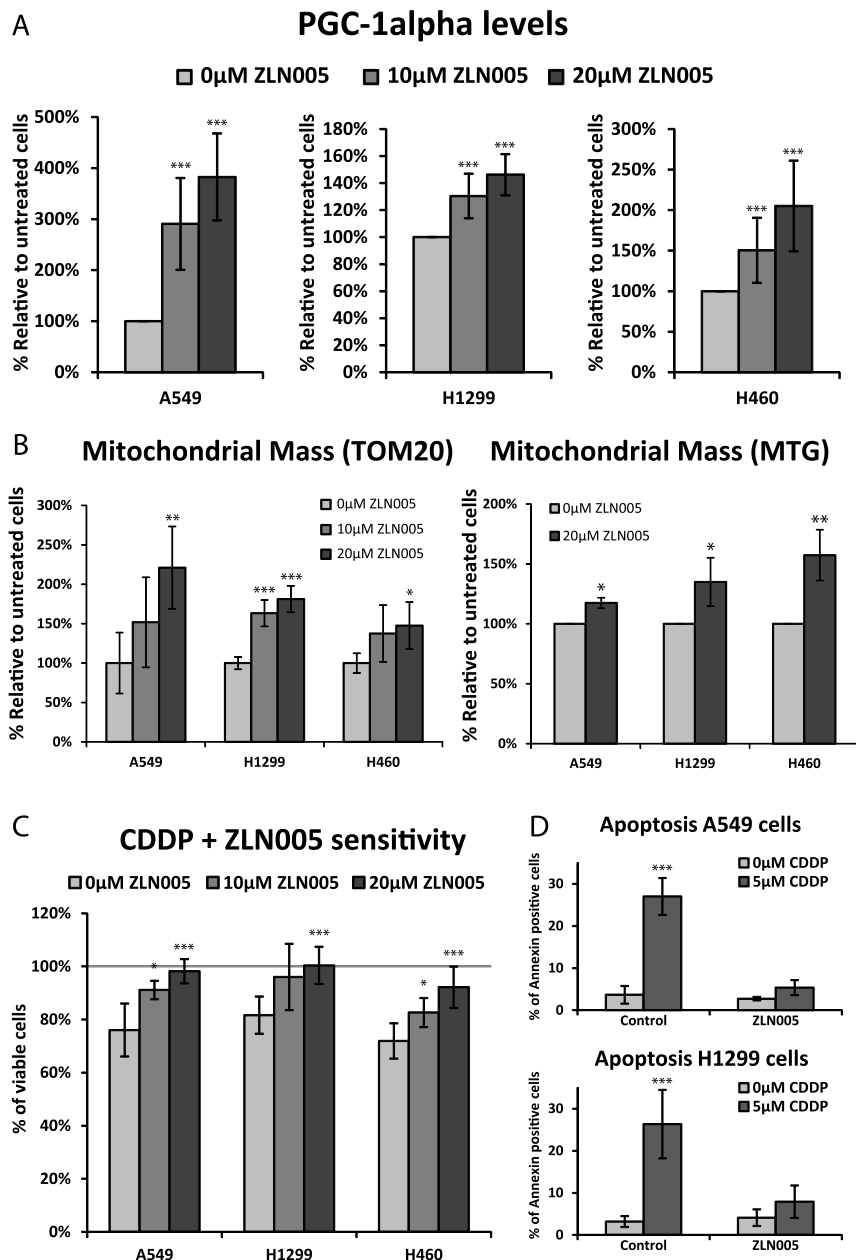


Fig. 6. ZLN005 treatment induces an increase in mitochondrial mass and reduces CDDP-sensitivity in cell lines. (A) ZLN005 treatment induces PGC-1 α mRNA levels (B) Mitochondrial mass measured by MTG and TOM20 IHC in ZLN005 treated cells for 48 h. Bars are means from at least three different experiments and are represented as percentage of untreated parental cells. ZLN005 reduces sensitivity to CDDP decreasing apoptosis. (C) Percentage of viable cells after 48 h of treatments. (D) Graph bars represent the mean percentage of Annexin positive cells from 4 measurements. Error bars indicate standard deviation. Student's t-test p-value was considered to be statistically significant when was < 0.05 (* = $P \leq 0.05$, ** = $P \leq 0.01$, *** = $P \leq 0.001$).

line; on the other side, no differences were seen for the line A549 CDDP resistant compared to its parental cell line.

In addition, we assessed the sensitivity of cell lines to rotenone, a specific inhibitor of mitochondrial Complex I and therefore of the OXPHOS function (Fig. 4F and Supplementary Figure 3). Similar to metformin, there are no significant differences in rotenone sensitivity between parental and CDDP-resistant A549 cells. However, the H1299 CDDP-resistant cells are significantly more sensitive to rotenone than their parental version.

3.5. Cisplatin treatment induces a cycle-independent, ROS-mediated, metabolic reprogramming

The results obtained with the resistant cell lines led us to wonder if these stable metabolic changes observed could be consequence of a selection process that happens during short time exposure to CDDP. In order to do so, we studied the early response to the drug. To simplify the interpretation of the results, only the statistical analysis between the

basal condition and after treatment is shown (Fig. 5). The remaining comparisons are shown in Supplementary Table 1.

Since PGC-1 α is induced by ROS, we studied whether cisplatin was able to increase cellular ROS levels. For this purpose, we analyzed the ROS levels 16 h after CDDP treatment in the different cell lines (Fig. 5A). The results showed an increase in ROS when the parental cells are treated with 5 μ M CDDP for 16 h. Similarly, this early change of ROS in response to treatment also occurs in resistant lines, which further augment their increased parameters. Therefore, this phenomenon seems to be common to parental and resistant cell lines. In addition, this confirms that the CDDP-resistant cell lines do not exhibit a more effective antioxidant response to CDDP treatment, which dismisses the possibility that their resistance is mediated by a reduction in oxidative damage.

Then we checked whether there was a process of metabolic reprogramming induced by short time CDDP treatment. We evaluated the levels of PGC1 α (Fig. 5B), mitochondrial mass (Fig. 5C) and MIMP (Fig. 5D) after 24 h of 5 μ M CDDP exposure. The results showed an

increase in all the parameters. Interestingly, this increase occurs in the three cell lines, although the CDDP-resistant line A549 does not have a stable increase in any of them.

In addition, this metabolic reprogramming induced by CDDP was avoided by antioxidant treatment. The simultaneous treatment with 10 mM *N*-Acetyl Cysteine (NAC) reduced the ROS levels in CDDP treated cells below controls. Curiously, in this situation the NAC treatment avoided the MIMP increase, indicating that this process is mediated by ROS (Fig. 5E).

On the other hand, since it is described that CDDP is an intercalating agent that hinders S phase, we tested if this MIMP increase at short times, could be the consequence of alterations in the cell cycle (Fig. 5F). Measuring the cell cycle we observed that, certainly, treatment with CDDP hold back cells in S-G2 phase, decreasing the proportion of cells in G1. However, this effect is lower in the resistant lines. Regarding the mitochondrial function, cells in S-G2 phase showed more MIMP, therefore part of the increase we saw is because the cells are detained in this phase. In any case, if we compare the cells within the same cell cycle phase, there is a cell-independent increase of MIMP during CDDP treatment.

3.6. Induction of PGC-1 α and mitochondrial mass by ZLN005 treatment reduces CDDP associated apoptosis

To isolate the effect of PGC-1 α increase from the rest of changes accumulated in the CDDP-resistant cells, we decided to treat the parental cells with the compound ZLN005 (a PGC-1 α transcriptional activator) to check if we could reproduce the CDDP resistant phenotype. This compound is described to increase PGC-1 α levels in muscle, however, no data exist for cancer cells [20].

Parental cell lines treated with ZLN005 increases their PGC-1 α mRNA levels in a dose-dependent manner at 48 h (Fig. 6A). Similarly, the ZLN005 treatment induces a rise in the levels of mitochondrial mass for the parental cell lines (Fig. 6B).

Next, we checked whether there was a reduction in the CDDP sensitivity associated to the induction of PGC-1 α and mitochondrial mass. The results show how ZLN005 treatment reduces CDDP sensitivity in a dose-dependent manner (Fig. 6C). Moreover, we analyzed the mechanism behind this reduction in CDDP sensitivity and we verified that apoptosis induced by CDDP was reduced by ZLN005 treatment (Fig. 6D and Supplementary Figure 4). Therefore, there is an association between the expression of PGC-1 α , the mitochondrial mass and the CDDP induced apoptosis.

3.7. Metabolic targeting with PGC-1 α siRNA or OXPHOS inhibitors in concomitance with CDDP in parental and CDDP resistant NSCLC cells

Since we saw an increase of OXPHOS function, also as an early response to CDDP treatment, and this metabolic reprogramming seems to be key for CDDP induced apoptosis, we tested if concomitant metabolic targeting of OXPHOS function through PGC-1 α siRNA, metformin or rotenone treatment might enhance the effect of cisplatin.

We proceeded in a similar manner, first we analyzed whether siRNA was able to reduce the early rise in MIMP induced by CDDP (Fig. 7A). The results show that PGC-1 α siRNA is able to control the increase of mitochondrial mass induced by cisplatin in the two lines A549 and H1299, for both parental and CDDP-resistant versions. Subsequently, we measured the cell viability using PGC-1 α siRNA in the presence of concomitant 5 μ M CDDP (Fig. 7B). Downregulation of PGC-1 α increases the effect of CDDP in all the cases. However, the differences in CDDP sensitivity between A549 parental and its CDDP-resistant version are maintained. On the other hand, due to an increased sensitivity to PGC-1 α downregulation in H1299 CDDP-resistant cells, the differences between parental and CDDP resistant H1299 cells are lost.

Secondly, we tested if metformin treatment was able to avoid the increase of MIMP produced by short time exposure to CDDP (Fig. 7C).

The metformin treatment restraint the MIMP rise induced by CDDP for all the cases. Furthermore, the treatment with metformin or rotenone eliminates the differences between parental and resistant cell lines to cisplatin treatment for both cell lines (Fig. 7D and E). The differences between parental and resistant cells are no longer significant from a concentration of 1 mM metformin or 1 nM rotenone for both A549 and H1299 cell lines.

4. Discussion

Cisplatin remains a cornerstone for treating NSCLC, however little is known about the mechanisms of resistance associated with changes in cell's metabolism. In this work, using cell models, PDX models and biopsies of patients with NSCLC, we have analyzed the metabolic changes produced by cisplatin treatment. In addition, taking advantage of these changes we have identified an increased sensitivity to OXPHOS inhibition or PGC-1 α interference in CDDP-resistant cell lines.

In our study, we generated resistant versions from three different cell lines after continued treatment with cisplatin for three months. Two out of three cell lines showed stable changes towards an increased OXPHOS function and reduced glycolysis (increased MIMP, galactose to glucose growth ratio, mitochondrial mass and oxygen consumption but reduced glucose consumption). However, the three of them responded in a similar way increasing ROS, MIMP and mitochondrial mass as an early response to CDDP treatment.

Interestingly, in our case, the metabolic changes were not associated with a more quiescent phenotype [21], since no stable changes were observed in the cell cycle phases. This opens up the possibility of changes in metabolism after chemotherapy, regardless of the increase in quiescent phenotype, as it has been described so far [12]. In order to check whether the mechanism of metabolism modification that we describe can be parallel to the typical alterations of proteins related to apoptosis, we have analyzed the levels of BCL2 and AIF (Supplementary Figure 5). As previously described, we saw a decrease in AIF (pro-apoptosis) and an increase in BCL2 (anti-apoptosis), which would indicate that our mechanism does not replace other classical mechanisms already described of cisplatin resistance [22].

PGC-1 α is the master regulator of mitochondrial biogenesis and metabolic energy metabolism. In our case we saw a stable increase of this transcriptional activator, precisely, in the two cell lines (H1299 and H460) that showed an increased OXPHOS function. In the same way, the CDDP-resistant A549 cell line, without changes observed in the OXPHOS function, did not show an increase in PGC-1 α expression.

Perhaps due to the difficulty of obtaining post-treatment re-biopsies in NSCLC, there is no literature that study this metabolism reprogramming after treatment in NSCLC biopsies. To solve this problem and confirm our results beyond the cell lines, we first decided to retrospectively analyze CDDP treated PDX models available in the laboratory. Similar to the results obtained in cell lines, the results in PDX models show an increase in PGC-1 α and mitochondrial mass, as well as a reduction of the GAPDH/MT-CO1 ratio mRNA levels, for two out of four PDX models.

Despite the difficulty of obtaining paired samples, we obtained enough biopsy material for the analysis in 3 patients. In all cases, we saw an increase in mitochondrial mass levels and a decrease in the GAPDH/MT-CO1 ratio, strongly suggesting a metabolic reprogramming towards a more oxidative metabolism [23]. Similar results have been observed in post-treatment tumor biopsies from colon cancer patients [24].

This metabolic change associated with the treatment could also have an implication in glucose uptake and therefore in PET imaging when evaluating the treatment response or the disease extent.

In our experience the resistant CDDP lines are less glycolytic, similarly in patients the post-neoadjuvant SUVmax is also lower. In addition, the post-treatment samples in both, the PDX and the patients, showed a decrease in the GAPDH/MT-CO1 ratio that has already been correlated with the levels of SUVmax in NSCLC [23]. Perhaps due to

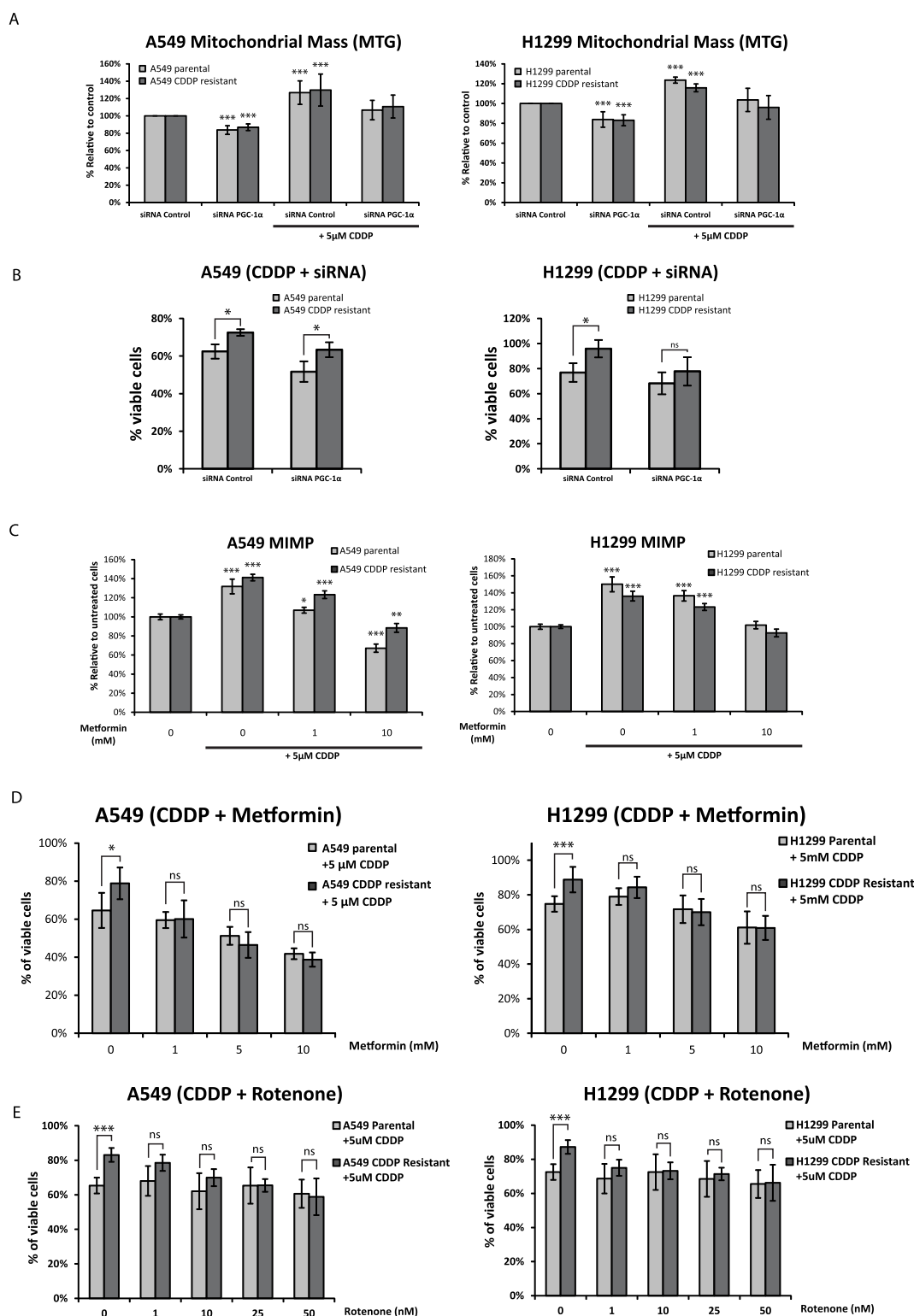


Fig. 7. Metabolic targeting in concomitance with CDDP in parental and CDDP resistant NSCLC cells. PGC-1 α siRNA reduces the MTG increase produced by CDDP (A). Effect of concomitant PGC-1 α siRNA interference on cell viability (B). Metformin treatment reduces the MIMP increase produced by CDDP treatment in both A549 and H1299 cell lines (C). Metformin and Rotenone eliminates the differences between parental and resistant cell lines to cisplatin treatment for both A549 and H1299 cells (D and E). The graphs represent the percentage of viable cells (Y-axis) after 48 h of different metformin or rotenone treatments (X-axis). Data are means from at least three different experiments and are represented as percentage of untreated cells. Error bars indicate standard deviation. Student's t-test p-value was considered to be statistically significant when was < 0.05 (* = $P \leq 0.05$, ** = $P \leq 0.01$, *** = $P \leq 0.001$).

this process of metabolism reprogramming in post-treatment cells (with an increase in mitochondrial function and a decrease in glucose consumption), the SUVmax post-treatment drop is not a prognostic factor,

as it would not be a good indicator of the pathological response [25].

All these results in different models and tumor biopsies indicate a process of metabolic reprogramming towards a greater OXPHOS

function against the Warburg Effect. Most tumor cells prefer using aerobic glycolysis despite the lower energy yield thereof (in comparison to the use of the more efficient OXPHOS system), since this “Warburg metabolism” is adapted to sustain exponential growth [11,26]. However, as our results indicate, there is an increase in OXPHOS function associated to CDDP treatment. A series of recent reports with similar results for other tumors strongly support our observations [24,27–33]. Similar to our results in NSCLC, it has been recently described how different cisplatin-resistant lung cancer cell lines showed a decreased glucose consumption with an increased OXPHOS function [34]. However, the authors describe an increase in glutamine dependence that we do not find in our CDDP-resistant cell lines (data not shown). Thus, to our knowledge, despite the importance of platinum treatments in NSCLC, this mechanism of metabolic reprogramming associated with CDDP resistance has not been demonstrated in this type of tumors until this study.

Regarding the mechanism, PGC-1 α can be triggered by oxidative damage and chemotherapy in cancer cells [35]. Supporting these results, we saw an increase in ROS and PGC-1 α shortly after treatment. Furthermore, treatment with the antioxidant NAC prevents the increase of ROS and the increase of mitochondrial function induced by CDDP, which would support that this metabolism reprogramming is induced by ROS.

In fact, treatment of parental cells with the PGC-1 α inducer ZLN005, reduces sensitivity to CDDP by increasing resistance to apoptosis. The increase of mitochondrial mass and OXPHOS performance has been associated with a reduction in treatment-induced apoptosis [28,36]. Since a loss of MIMP is key for apoptosis triggering, a strong possibility would be that the higher MIMP would withstand better possible fluctuations in this parameter and then hamper the apoptosis triggering. Besides that, cisplatin binds with greater affinity to mtDNA compared to nuclear DNA. Thus, having higher levels of mitochondrial mass would reduce the CDDP toxic effect on the cell [37].

Our hypothesis is that these mechanisms, as well as others yet to be fully explored, would produce under short-term treatment an advantage for cells with an increased OXPHOS phenotype, which in the long-term treatment scenario would lead to cells with a stable increased OXPHOS function (Fig. 8).

On the other hand, PGC-1 α is also involved in the antioxidant response, controlling the expression of detoxifying enzymes [38]. Increased antioxidant response mediated by PGC-1 α has been described as a mechanism of treatment resistance in melanoma and ovarian cancer [24,39–41]. However, in our case, the ROS levels measured with DCFHDA were significantly increased in all the CDDP-resistant cell lines. Remarkably, the ROS increase occurs both, as a stable modification in CDDP-resistant cell lines and also as an early response to short cisplatin exposure in all of the cell lines studied. Thus, in our experience, it appears that PGC-1 α levels do not have sufficient influence on ROS detoxification during CDDP treatments, making it difficult to hypothesize a greater tolerance to CDDP-induced oxidative stress in resistant lines as the main mechanism of CDDP resistance. As a matter of fact, the increase of ROS correlates with the reduction of apoptosis in

different scenarios [8,42,43].

In addition, we investigated if this group of resistant cells with enhanced OXPHOS could be targeted inhibiting the mitochondrial function by means of different treatments (Metformin, Rotenone and PGC-1 α siRNA) and under different approaches (alone or in concomitance with CDDP).

We demonstrated that both, the silencing of PGC-1 α and the treatment with the mitochondrial inhibitors metformin or rotenone reduced the viability of the cell lines proportionally to their OXPHOS requirements. Thereby, the reduction was greater in the H1299 CDDP-resistant cell line, in which an increase of the OXPHOS function, compared to the parental version, was observed. However, the A549 CDDP-resistant line, for which no increase in any OXPHOS parameter was observed, maintained the same profile of sensitivity to the different treatments.

On the other hand, the concomitant treatment of CDDP with metformin, rotenone or the silencing of PGC-1 α increases the effect of CDDP in all cases. In fact, the combined therapy of metformin or rotenone with CDDP eliminates the differences of sensitivity between parental and resistant lines for both A549 and H1299 cell lines. Likewise, the combined therapy of PGC-1 α siRNA and CDDP eliminates the differences of sensitivity between parental and resistant lines for the H1299 line but not for the A549 line.

Metformin is a drug commonly used for its antidiabetic properties, although in the last years it has aroused an interest for its antitumor role [44]. Regarding to bioenergetics, it has recently been described that metformin inhibits the Complex I of the mitochondrial electron transport chain [45] and reduces the flow of glucose- and glutamine-derived metabolic intermediates into the tricarboxylic acid cycle [46]. Compatible with this, our study showed that the addition of metformin decreases the MIMP, thus explaining the differential sensitivity between the cell lines. The similar results between the effect of rotenone and metformin reinforce the CI inhibition mechanism of metformin over other non-OXPHOS effects. There are numerous retrospective studies in different tumor types including NSCLC, which support the antitumor role of metformin and its relationship with chemoradiotherapy treatments [47,48]. A possible explanation for the best prognosis of cancer patients taking metformin, could be due to its role as OXPHOS inhibitor which is key, as our findings indicate, for the chemotherapy resistance phenotype.

5. Conclusion

In summary, an increase in the mitochondrial mass, and therefore OXPHOS function, is a recurrent mechanism of resistance to cisplatin treatment in NSCLC. Importantly, this characteristic of cisplatin-resistant cells can be therapeutically used through the inhibition of PGC-1 α or the use of mitochondrial inhibitors. In any case, this metabolic reprogramming does not occur in all the cases analyzed, being necessary the validation of predictive markers of this resistance process. This would be key for the success of future clinical trials since would allow the identification of patients who would benefit from metabolism targeted treatments.

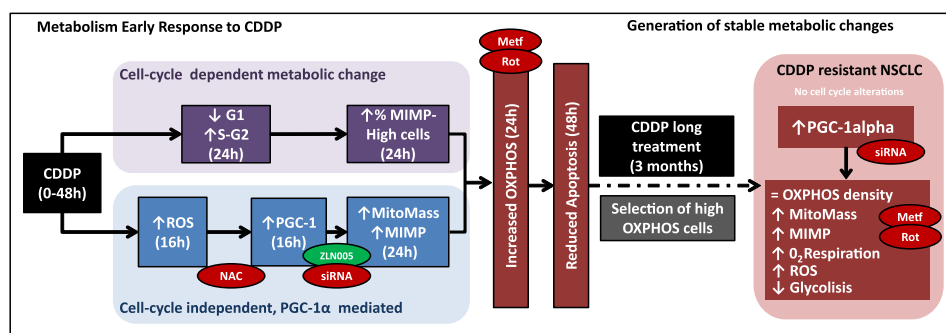


Fig. 8. Proposed metabolic reprogramming model associated to CDDP treatment in NSCLC. Short-term changes (Left side) and Long-term changes (Right side) are shown. Cells with increased mitochondrial Mass and OXPHOS function are selected during short exposure to CDDP leading to stable OXPHOS changes during long term treatment. The ellipses show the pharmacological or genomic approaches used in this study that block (in red) or increase (in green) this mechanism. NAC: N-Acetyl Cysteine, Metf: Metformin, Rot: Rotenone, siRNA: PGC-1 α siRNA.

Ethics approval and consent to participate

All the experiments carried out in this study complied with current Spanish and European Union laws and the principles outlined in the Declaration of Helsinki. The study and experimental protocols involving patient samples or animals were approved by the Hospital Universitario Puerta de Hierro Ethics Committee. Written informed consent was obtained from all the patients recruited.

Consent for publication

Not applicable.

Availability of data and materials

The datasets used and analyzed during the current study are available from the corresponding author on reasonable request.

Conflicts of interest

The authors declare that there are no known conflicts of interest associated with this publication and there has been no significant financial support for this work that could have influenced its outcome.

Authors' contributions

A.C-B and M.P conceived the study. A.C-B, A.G-G, S.L-M, A.R, P.M-A, and J.M.G designed the experiments. A.C-B, R.L-B, R.J.V-B, A.G-G, M.J-C, S.P-Z, M.R.M-V, C.L, C.A, A.M-R, and C.S performed the experiments. A.C-B, F.F, V.C, C.A, A.R, and J.M.G analyzed the data. A.C-B, M.P, R.L-B, S.L-M and J.M.G wrote the paper. All authors read and approved the final manuscript.

Acknowledgments

Not applicable.

Funding

Work in the authors' laboratories is supported by "Instituto de Salud Carlos III" PI13/01806 and PIE14/0064 to M.P. A.C-B, received a Spanish Lung Cancer Group fellowship. R.L-B, is supported by Comunidad Autónoma de Madrid "Garantía juvenil" contract.

Appendix A. Supplementary data

Supplementary data to this article can be found online at <https://doi.org/10.1016/j.freeradbiomed.2019.03.009>.

References

- [1] J. Vansteenkiste, D. De Ruyscher, W.E.E. Eberhardt, E. Lim, S. Senan, E. Felip, et al., Early and locally advanced non-small-cell lung cancer (NSCLC): ESMO Clinical Practice Guidelines for diagnosis, treatment and follow-up, *Ann. Oncol.* 24 (Suppl 6) (2013) vi89–98, <https://doi.org/10.1093/annonc/mdt241>.
- [2] S. Novello, F. Barlesi, R. Califano, T. Cufer, S. Ekman, M.G. Levrá, et al., Metastatic non-small-cell lung cancer: ESMO Clinical Practice Guidelines for diagnosis, treatment and follow-up, *Ann. Oncol.* 27 (2016) V1–V27, <https://doi.org/10.1093/annonc/mdw326>.
- [3] A. Custodio, M. Méndez, M. Provencio, Targeted therapies for advanced non-small-cell lung cancer: current status and future implications, *Cancer Treat Rev.* 38 (2012) 36–53, <https://doi.org/10.1016/j.ctrv.2011.04.001>.
- [4] F. Tartari, M. Santoni, L. Burattini, P. Mazzanti, A. Onofri, R. Berardi, Economic sustainability of anti-PD-1 agents nivolumab and pembrolizumab in cancer patients: Recent insights and future challenges, *Cancer Treat Rev.* 48 (2016) 20–24, <https://doi.org/10.1016/j.ctrv.2016.06.002>.
- [5] D.A. Fennell, Y. Summers, J. Cadranet, T. Benepal, D.C. Christoph, R. Lal, et al., Cisplatin in the modern era: The backbone of first-line chemotherapy for non-small cell lung cancer, *Cancer Treat Rev.* 44 (2016) 42–50, <https://doi.org/10.1016/j.ctrv.2016.01.003>.
- [6] D. Hanahan, R.A. Weinberg, Hallmarks of cancer: the next generation, *Cell* 144 (2011) 646–674, <https://doi.org/10.1016/j.cell.2011.02.013> S0092-8674(11)00127-9 [pii].
- [7] E. Obre, R. Rossignol, Emerging concepts in bioenergetics and cancer research: Metabolic flexibility, coupling, symbiosis, switch, oxidative tumors, metabolic remodeling, signaling and bioenergetic therapy, *Int. J. Biochem. Cell Biol.* 59 (2015) 167–181, <https://doi.org/10.1016/j.biocel.2014.12.008>.
- [8] A. Cruz-Bermúdez, R.J. Vicente-Blanco, E. Gonzalez-Vioque, M. Provencio, M.Á. Fernández-Moreno, R. Garesse, Spotlight on the relevance of mtDNA in cancer, *Clin. Transl. Oncol.* (2016) 1–10, <https://doi.org/10.1007/s12094-016-1561-6>.
- [9] S. Vyas, E. Zaganjor, M. Haigis, Mitochondria and cancer, *Cell* 166 (2016) 555–566, <https://doi.org/10.1016/j.molcel.2016.02.011>.
- [10] O. Warburg, F. Wind, E. Negelein, The metabolism of tumors in the body, *J. Gen. Physiol.* 8 (1927) 519–530 <http://www.ncbi.nlm.nih.gov/pubmed/19872213>.
- [11] M. Vander Heiden, L. Cantley, C. Thompson, Understanding the Warburg effect: the metabolic requirements of cell proliferation, *Science* 80 (324) (2009) 1029–1034 <http://www.sciencemag.org/content/324/5930/1029.short>, Accessed date: 24 April 2015.
- [12] D.A. Wolf, Is reliance on mitochondrial respiration a “chink in the armor” of therapy-resistant cancer? *Cancer Cell* 26 (2014) 788–795, <https://doi.org/10.1016/j.cccell.2014.10.001>.
- [13] J. Yoshida, Metabolic reprogramming: the emerging concept and associated therapeutic strategies, *J. Exp. Clin. Cancer Res.* 34 (2015) 111, <https://doi.org/10.1186/s13046-015-0221-y>.
- [14] H. Noto, A. Goto, T. Tsujimoto, M. Noda, Cancer risk in diabetic patients treated with metformin: A systematic review and meta-analysis, *PLoS One* 7 (2012) 1–9, <https://doi.org/10.1371/journal.pone.0033411>.
- [15] A.B. Parikh, P. Kozuch, N. Rohs, D.J. Becker, B.P. Levy, Metformin as a Repurposed Therapy in Advanced Non-small Cell Lung Cancer (NSCLC): Results of a Phase II Trial, (2017), <https://doi.org/10.1007/s10637-017-0511-7>.
- [16] R. Pello, M. a Martín, V. Carelli, L.G. Nijtmans, A. Achilli, M. Pala, et al., Mitochondrial DNA background modulates the assembly kinetics of OXPHOS complexes in a cellular model of mitochondrial disease, *Hum. Mol. Genet.* 17 (2008) 4001–4011, <https://doi.org/10.1093/hmg/ddn303>.
- [17] I. Wittig, H.P. Braun, H. Schägger, Blue native PAGE, *Nat. Protoc.* 1 (2006) 418–428, <https://doi.org/10.1038/nprot.2006.62>.
- [18] S. Soes, B.S. Sørensen, J. Alsner, J. Overgaard, H. Hager, L.L. Hansen, et al., Identification of accurate reference genes for RT-qPCR analysis of formalin-fixed paraffin-embedded tissue from primary non-small cell lung cancers and brain and lymph node metastases, *Lung Canc.* 81 (2013) 180–186, <https://doi.org/10.1016/j.lungcan.2013.04.007>.
- [19] A. Calles, B. Rubio-Viqueira, M. Hidalgo, Primary human non-small cell lung and pancreatic tumour models—utility and applications in drug discovery and tumor biology, *Curr. Protoc. Pharmacol.* (2013) 1–21, <https://doi.org/10.1002/0471141755.ph1426s61> Chapter 14.
- [20] L.N. Zhang, H.Y. Zhou, Y.Y. Fu, Y.Y. Li, F. Wu, M. Gu, et al., Novel small-molecule PGC-1α transcriptional regulator with beneficial effects on diabetic db/db mice, *Diabetes* 62 (2013) 1297–1307, <https://doi.org/10.2337/db12-0703>.
- [21] A. Roesch, A. Vultur, I. Bogeski, H. Wang, K. Zimmermann, D. Speicher, et al., Overcoming intrinsic multidrug resistance in melanoma by blocking the mitochondrial respiratory chain of slow-cycling JARID1Bhigh cells, *Cancer Cell* 23 (2013) 811–825, <https://doi.org/10.1016/j.ccr.2013.05.003>.
- [22] L. Galluzzi, L. Senovilla, I. Vitale, J. Michels, I. Martins, O. Kepp, et al., Molecular mechanisms of cisplatin resistance, *Oncogene* 31 (2012) 1869–1883, <https://doi.org/10.1038/onc.2011.384>.
- [23] A. Cruz-Bermúdez, R.J. Vicente-Blanco, R. Laza-Briviesca, A. García-Grande, S. Laine-Menéndez, L. Gutiérrez, et al., PGC-1α levels correlate with survival in patients with stage III NSCLC and may define a new biomarker to metabolism-targeted therapy, *Sci. Rep.* 7 (2017), <https://doi.org/10.1038/s41598-017-17009-6>.
- [24] T.T. Vellinga, V.C.J. De Boer, S. Fatrai, S. Van Schelven, K. Trumpi, A. Verheem, et al., SIRT1/PGC1α-Dependent increase in oxidative phosphorylation supports chemotherapy resistance of colon cancer, *Clin. Cancer Res.* 21 (2015) 2870–2879, <https://doi.org/10.1158/1078-0432.CCR-14-2290>.
- [25] J.K. Park, J.J. Kim, S.W. Moon, Variations in positron emission tomography-computed tomography findings for patients receiving neoadjuvant and non-neoadjuvant therapy for non-small cell lung cancer, *J. Thorac. Dis.* 9 (2017) 344–354, <https://doi.org/10.21037/jtd.2017.02.38>.
- [26] P.S. Ward, C.B. Thompson, Metabolic reprogramming: A cancer hallmark even Warburg did not anticipate, *Cancer Cell* 21 (2012) 297–308, <https://doi.org/10.1016/j.ccr.2012.02.014>.
- [27] L.E. Brace, S.C. Vose, K. Stanya, R.M. Gathungu, V.R. Marur, A. Longchamp, et al., Increased oxidative phosphorylation in response to acute and chronic DNA damage, *NPJ Aging Mech. Dis.* 2 (2016) 16022, <https://doi.org/10.1038/npjamd.2016.22>.
- [28] N. Yadav, S. Kumar, T. Marlowe, A.K. Chaudhary, R. Kumar, J. Wang, et al., Oxidative phosphorylation-dependent regulation of cancer cell apoptosis in response to anticancer agents, *Cell Death Dis.* 6 (2015), <https://doi.org/10.1038/cddis.2015.305> e1969-13.
- [29] M.V. Shirmanova, I.N. Druzhkova, M.M. Lukina, V.V. Dudenkova, N.I. Ignatova, L.B. Snopova, et al., Chemotherapy with cisplatin: Insights into intracellular pH and metabolic landscape of cancer cells in vitro and in vivo, *Sci. Rep.* 7 (2017) 1–13, <https://doi.org/10.1038/s41598-017-09426-4>.
- [30] M. Gabrielson, M.Y. Björklund, J. Carlson, M. Shoshan, Expression of mitochondrial regulators PGC1α and TFAM as putative markers of subtype and chemoresistance in epithelial ovarian carcinoma, *PLoS One* 9 (2014), <https://doi.org/10.1371/journal>.

- pone.0107109.
- [31] C. Denise, P. Paoli, M. Calvani, M.L. Taddei, E. Giannoni, S. Kopetz, et al., 5-Fluorouracil resistant colon cancer cells are addicted to OXPHOS to survive and enhance stem-like traits, *OncoTarget* 6 (2015) 41706–41721, <https://doi.org/10.18632/oncotarget.5991>.
 - [32] P.S. Thiagarajan, X. Wu, W. Zhang, I. Shi, R. Bagai, P. Leahy, et al., Transcriptomic-metabolomic reprogramming in EGFR-mutant NSCLC early adaptive drug escape linking TGFβ2-bioenergetics-mitochondrial priming, *OncoTarget* (2016), <https://doi.org/10.18632/oncotarget.13307>.
 - [33] D.S. Matassa, M.R. Amoroso, H. Lu, R. Avolio, D. Arzeni, C. Procaccini, et al., Oxidative metabolism drives inflammation-induced platinum resistance in human ovarian cancer, *Cell Death Differ.* (2016) 1–13, <https://doi.org/10.1038/cdd.2016.39>.
 - [34] M. Wangpaichitr, C. Wu, Y.Y. Li, D.J.M. Nguyen, S. Shah, S. Chen, et al., Exploiting ROS and Metabolic Differences to Kill Cisplatin Resistant Lung Cancer vol. 8, (2017), pp. 49275–49292.
 - [35] Z. Tan, X. Luo, L. Xiao, M. Tang, A.M. Bode, Z. Dong, et al., The role of PGC1 in cancer metabolism and its therapeutic implications, *Mol. Canc. Therapeut.* 15 (2016) 774–782, <https://doi.org/10.1158/1535-7163.MCT-15-0621>.
 - [36] M. Wintzell, L. Löfstedt, J. Johansson, A.B. Pedersen, J. Fuxe, M. Shoshan, Repeated cisplatin treatment can lead to a multiresistant tumor cell population with stem cell features and sensitivity to 3-bromopyruvate, *Cancer Biol. Ther.* 13 (2012) 1454–1462, <https://doi.org/10.4161/cbt.22007>.
 - [37] Z. Yang, L.M. Schumaker, M.J. Egorin, E.G. Zuhowski, Z. Quo, K.J. Cullen, Cisplatin preferentially binds mitochondrial DNA and voltage-dependent anion channel protein in the mitochondrial membrane of head and neck squamous cell carcinoma: Possible role in apoptosis, *Clin. Cancer Res.* 12 (2006) 5817–5825, <https://doi.org/10.1158/1078-0432.CCR-06-1037>.
 - [38] J. St-Pierre, J. Lin, S. Krauss, P.T. Tarr, R. Yang, C.B. Newgard, et al., Bioenergetic analysis of peroxisome proliferator-activated receptor γ coactivators 1 α and 1 β (PGC-1 α and PGC-1 β) in muscle cells, *J. Biol. Chem.* 278 (2003) 26597–26603, <https://doi.org/10.1074/jbc.M301850200>.
 - [39] B. Kim, J.W. Jung, J. Jung, Y. Han, D.H. Suh, H.S. Kim, et al., PGC1 α induced by reactive oxygen species contributes to chemoresistance of ovarian cancer cells, *OncoTarget* 8 (2017) 60299–60311, <https://doi.org/10.18632/oncotarget.19140>.
 - [40] F. Vazquez, J.H. Lim, H. Chim, K. Bhalla, G. Girnun, K. Pierce, et al., PGC1 α expression defines a subset of human melanoma tumors with increased mitochondrial capacity and resistance to oxidative stress, *Cancer Cell* 23 (2013) 287–301, <https://doi.org/10.1016/j.ccr.2012.11.020>.
 - [41] D. Cao, L. Jin, H. Zhou, W. Yu, Y. Hu, T. Guo, Inhibition of PGC-1 α after chemotherapy-mediated insult confines multiple myeloma cell survival by affecting ROS accumulation, *Oncol. Rep.* 33 (2015) 899–904, <https://doi.org/10.3892/or.2014.3635>.
 - [42] A. Cruz-Bermúdez, C. Vallejo, R.J. Vicente-blanco, M.E. Gallardo, M.A. Fernandez-Moreno, M. Quintanilla, et al., Enhanced tumorigenicity by mitochondrial DNA mild mutations, *OncoTarget* 6 (2015) 13628–13643 <http://www.ncbi.nlm.nih.gov/pubmed/25909222>, Accessed date: 6 June 2015.
 - [43] M. Redza-Dutordoir, D.A. Averill-Bates, Activation of apoptosis signalling pathways by reactive oxygen species, *Biochim. Biophys. Acta Mol. Cell Res.* 1863 (2016) 2977–2992, <https://doi.org/10.1016/j.bbamcr.2016.09.012>.
 - [44] R.-H. Tian, Y.-G. Zhang, Z. Wu, X. Liu, J.-W. Yang, H.-L. Ji, Effects of metformin on survival outcomes of lung cancer patients with type 2 diabetes mellitus: a meta-analysis, *Clin. Transl. Oncol.* 18 (2016) 641–649, <https://doi.org/10.1007/s12094-015-1412-x>.
 - [45] W.W. Wheaton, S.E. Weinberg, R.B. Hamanaka, S. Soberanes, L.B. Sullivan, E. Anso, et al., Metformin Inhibits Mitochondrial Complex I of Cancer Cells to Reduce Tumorigenesis, (2014), pp. 1–18, <https://doi.org/10.7554/eLife.02242>.
 - [46] T. Griss, E.E. Vincent, R. Egnatchik, J. Chen, E.H. Ma, B. Faubert, et al., Metformin antagonizes cancer cell proliferation by suppressing mitochondrial-dependent biosynthesis, *PLoS Biol.* 13 (2015), <https://doi.org/10.1371/journal.pbio.1002309>.
 - [47] K.C.J. Wink, J.S.A. Belderbos, E.M.T. Dieleman, M. Rossi, C.R.N. Rasch, R.A.M. Damhuis, et al., Improved progression free survival for patients with diabetes and locally advanced non-small cell lung cancer (NSCLC) using metformin during concurrent chemoradiotherapy, *Radiother. Oncol.* 118 (2016) 453–459, <https://doi.org/10.1016/j.radonc.2016.01.012>.
 - [48] C. Coyle, F.H. Cafferty, C. Vale, R.E. Langley, Metformin as an adjuvant treatment for cancer: a systematic review and meta-analysis, *Ann. Oncol. Off. J. Eur. Soc. Med. Oncol.* (2016) 1–12, <https://doi.org/10.1093/annonc/mdw410>.